EIGENSTRAIN GENERATED BY SHOT PEENING IN UDIMET 720LI INFERRED BY MEANS OF FINITE ELEMENT AND ANALYTICAL MODELS.

M.Satraki[1,2], A.Evans[2,3], A.King[3], G.Bruno[2,3], P.J Withers[3]

[1] National Technical University of Athens, Iroon Polytexneiou 9,15780 Zografou, Greece
[2] Institut Laue-Langevin, 6 rue Jules Horowitz, BP156, 38042 Grenoble, France
[3] Materials Science Centre, University of Manchester, Manchester, M1 7HS, UK

ABSTRACT

The residual stress in shot peened Udimet 720Li was determined by laboratory X-ray diffraction measurements. Depth profiles were obtained by electrochemical layer removal and a tensile peak was observed sub surface. A correction for layer removal was applied and the corrected data has been used to calculate the profile of the eigenstrain necessary to generate such a residual stress profile. Calculations were made applying two methods: 1) A Finite Element Model (FEM) using a thermally driven expansion to simulate the eigenstrain, 2) A simple analytical model. The latter took into account strain hardening, as measured in fatigue tests, and stress balance. Using the eigenstrain profile, the geometrically necessary cold work stored in the component was calculated. Results show a very good agreement between the two different models. The analytical method predicts a compressive misfit, while this was explicitly discarded in the FEM model. The calculated cold work is essentially the same for both models, but shows different behaviour from the peak integral width.

Subject Index: Udimet 720Li, Residual stress, eigenstrain, cold work, modelling

INTRODUCTION

It is well known that the residual stress state and cold work introduced by shot peening can improve the fatigue performance when the process is optimised. The residual stress state is created by the incompatibility between the plastically deformed zone around the indent of the impinging shot, and the surrounding elastically deformed region. The residual stress field is dependent upon the sample geometry and the induced plastic strain. Except for very thin sections and sharp radii, this plastic, non-compatible strain, termed the "eigenstrain", is assumed to be essentially independent of the sample geometry. By understanding the relationship between shot peening and the eigenstrain distribution it would be possible to predict the residual stress distribution in different object geometries and process optimisation. The modelling of the shot peening process has been explored by many authors (Schiffer, 1999, Meguid, 2002). Efforts have been made to understand the generation of the plastic zone and residual stress field through the deformation of a contacting body. Models have considered both quasi-static and dynamic loads (Schiffer, 1999). Considering models with multiple impacts, results have shown the equivalent plastic strain (which appears to be equivalent to the eigenstrain) to be tensile and to extend up to the depth of maximum balancing tensile stress [Meguid, 2002]. Another approach, outlined in (Korsunsky, 1997), was to calculate the resulting residual stress state following peening by analytical modelling of the eigenstrain distribution and component bending. The eigenstrain is found as bell shaped, decreasing to zero at the depth of the maximum calculated balancing tensile residual stress [http, 2000]. The aim of the present work was to determine the necessary eigenstrain distribution needed to generate a residual stress profile measured (by X-ray diffraction) in shot peened Udimet 720Li. Two approaches are presented: the finite element method using thermal expansion as a device to create the eigenstrain, and an analytical approach creating the eigenstrain by elasto-plastic deformation with strain hardening.

EXPERIMENTAL RESULTS

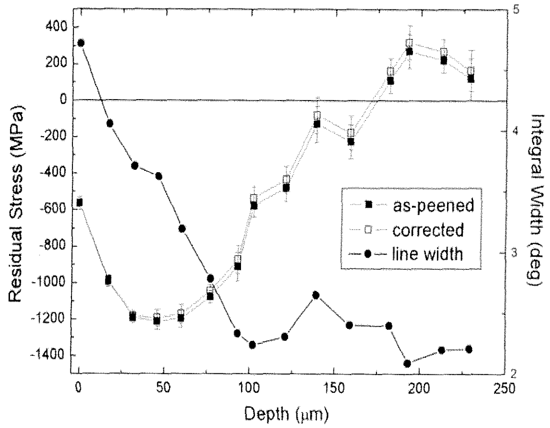

Fig.1- Experimental data for integral width and residual stresses as a function of the depth before and after correction for layer removal, (Kim, 2004).

A Udimet 720Li plate of dimensions 28×28×10 mm^3 was shot peened on both sides (see (Kim, 2004) for full details). The residual stress depth profiles were recorded by a lab X-ray diffractometer using the layer removal technique. Details are given in (Kim, 2004). The stress was calculated based upon the $\sin^2\psi$ technique, using a simplified Dölle-Hauk method (Noyan, 1987). The peak width w was determined directly as the standard deviation of the Gaussian fit of a diffraction peak. Measurements were carried out in 20-30 μm steps to a depth of about 250 μm, see (Kim, 2004). Correction for layer removal was carried out using classical formulae (Moore and Evans, 1958), which depend on the effective sample thickness. In this case, the sample was peened on both front and back faces but the total thickness of 10 mm was considered. Fig.1 shows the results obtained: as one would expect the correction increases the tensile balancing stress slightly and shifts the point of inversion from compression to tension about 10 μm towards the surface. Although this correction lies within the experimental uncertainty, the corrected values were used for the following simulations.

THEORETICAL METHODS

Both our modelling approaches consider the peened states as arising from a single deformation event. In reality, the shot peening process is obviously progressive and it yields redundant deformation, resembling to some extent to low cycle fatigue loading.

Finite Element Modelling (FEM)

A Finite Element (FE) model has been used to iteratively back-calculate (i.e. infer from the experimental data) the eigenstrain induced in the surface by the mechanical deformation arising from shot peening. In practice, thermal expansion was used as a device to simulate the eigenstrain. By imposing a temperature profile with depth from the surface it was possible to generate the eigenstrain using an in-plane coefficient of thermal expansion of 1×10^{-6} /K (zero out-of-plane). This process was iterated until the residual strain along a particular direction as calculated by the FEM agreed with the experimental residual strain, as deduced from the experimental RS (Fig.1) using 2-D formulae. The agreement implied that the thermal gradient and hence the inferred eigenstrain was appropriate. The starting point of the iterative process (first approximation for the thermal profile) was an unconstrained strain profile. The latter was deduced by the subtraction of the flat balancing bulk tension from the total corrected residual stress profile shown in Fig.1. Bending was neglected since the sample had been shot peened on opposite faces. The Finite Element (FE) calculations were performed in ABAQUS. The FE mesh was created in the Patran software. The mesh used for the FE modelling was taken as 1/8 of the whole sample, i.e. 14x14x5 mm^3 (x, y, z). The nodes were homogeneously spaced in the xy plane in 1mm steps. In the z direction the nodes were spaced at increasing steps, from 0.02 mm at the surface to 1mm in the bulk. Symmetric boundary conditions were fixed at all internal surfaces. The external surfaces were kept fixed. The thermal gradient was applied to all nodes from the peened surface up to 0.5mm depth and only elastic deformation was considered. The elastic constants were: E= 208 GPa and ν= 0.31 corresponding to Ni-base Udimet 720Li superalloy. The deformation process was assumed to be static.

Analytical modelling

The biaxial plastic stress is given by

$$\sigma^{pl}(z) = \alpha E \varepsilon^{pl}(z) \qquad (1)$$

where $\alpha = 1/(1-\nu)$, E the Young's modulus and ν the Poisson's ratio.

In the case of a doubly peened slab, moment balance is automatically fulfilled: the two bending moments ($M = d\sigma/dz$) due to peening of each surface cancel each other and the elastic balancing stress must have a constant profile.

Now, if we apply stress balance, the stress over the whole slab thickness 2t is

$$\sigma(z) = \alpha E \left\{ \varepsilon^{pl}(z) - \frac{1}{t}\int_0^t \varepsilon^{pl}(z')dz' \right\} \qquad (2)$$

This result is consistent with the fact that in the elastic region, where $\varepsilon^p(z) = 0$, we will have the constant balancing stress:

$$\sigma_A = -\frac{\alpha E}{t}\int_0^t \varepsilon^{pl}(z')dz' \qquad (3)$$

To determine the profile of $\varepsilon^p(z)$ we just need to discretise the integral equation (2), because we know $\sigma(z)$ in N points (the measured profile). This will lead to a linear system of the kind:

$$\begin{cases} \sigma(z_1) = \alpha E \left\{ \varepsilon^{pl}(z_1) - \dfrac{1}{w} \sum_{i=1}^{N} \varepsilon^{pl}(z_i) \Delta z_i \right\} \\ \quad\quad\quad\quad .... \\ \sigma(z_N) = \alpha E \left\{ \varepsilon^{pl}(z_N) - \dfrac{1}{w} \sum_{i=1}^{N} \varepsilon^{pl}(z_i) \Delta z_i \right\} \end{cases} \quad (4)$$

in which the unknowns are simply $\varepsilon^{p}(z_i)$, i = 1,N. Since the intervals Δz_i and the values $\sigma(z_i)$ are all known. The start of the elastic region will be visible only if the data are collected up to a depth large enough to see it. In our case this was not done.

At this point, the total strain input during peening ε^{T} could be calculated assuming a bilinear hardening law in the plastic region (see Fig.2): it could be modelled as the sum of the plastic strain ε^{pl}, the macroscopic strain ε_A representing the final unconstrained deformation of the component, and an elastic strain, which is released upon unloading. Fig.2 shows this model for a one-dimensional case. In our case, the same model can be used, taking care of using the Von Mises equivalent stress (and yield strength). In our case $\sigma_1 = \sigma_2$ and $\sigma_3 = 0$, so that $\sigma_{VM} = \sigma_1$ and the yield criterion reads $\sigma_{VM} = \sigma'_y/= \sigma_y/\sqrt{2}$.

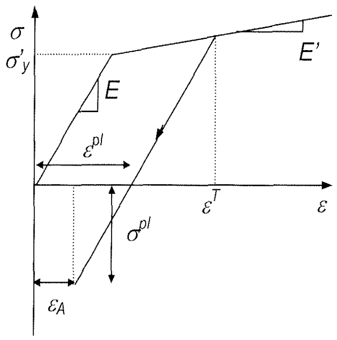

Fig.2. The stress-strain model used in the analytical approach: elastic with linear strain hardening defining relevant variables. Experimentally determined values for Young's modulus E and the strain hardening coefficient E' were used (Kim, 2004).

In the bilinear case, the total strain input is, therefore:

$$\varepsilon_T = \frac{\sigma_y'}{E} + \frac{E\varepsilon^{pl}}{E - E'} \quad (5)$$

Finally, the cold work was calculated using the entire area under the σ-ε curve including the work associated to the residual stress (see Fig.2).

RESULTS AND DISCUSSION

The results obtained with the two approaches are shown in Fig.3.a and b. The eigenstrain profiles show very good agreement in the tensile region. The analytical method predicts a compressive peak at a depth similar to that found for the tensile stress peak. The FE method used to extract the eigenstrain profile would also predict such compressive peak. However, in order to understand whether the tensile peak is a geometric artefact, only positive eigenstrains were considered in the FE calculations. The balancing RS in the elastic regions are essentially identical. Since the tensile subsurface peak is predicted by the analytical model and not by the FE presented, it can be concluded that this peak is indeed generated by compressive plastic strains. In fact, although this misfit strain compressive peak (or residual stress tensile peak) has not been predicted by other theoretical (Meguid, 1999) and experimental works (Menig, 2003), neutron diffraction (Ezeilo, 2003) clearly shows that the tensile stress peak is not an effect of the layer removal. The contradiction between (Menig, 2003) and (Ezeilo, 2003) can be explained by the very different plate thickness (much bigger for the latter and comparable with the present case).

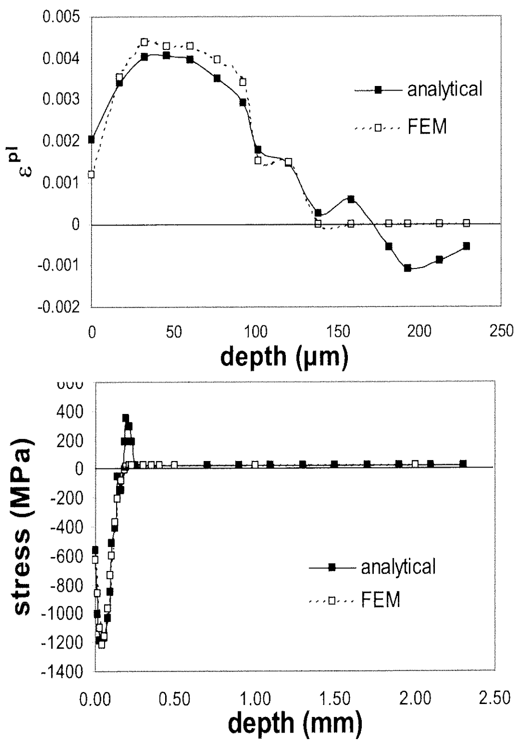

Fig.3. The results of the simple analytical and the FE model.
The misfit deformation follows the RS profile (a), but it is tensile where the RS is compressive. The re-calculated stress (b) has a balancing constant stress. The depth of the plastically deformed region can only be extrapolated from the data in (b).

The elastic region commences at two different depths, which can be evaluated upon extrapolation of the plastic strain or the residual stress profile: their values are 250 μm for the analytical model and 140 μm for the FE analysis.
The cold work was calculated as described above. Also for the FEM results, a bilinear material behaviour was taken (see Fig.2). The results could be compared with the integral width, which gives an indication of the cold work. This is shown in Fig.4, where the normalised quantities are reported. The behaviour of the modelled cold work is consistent with Fig.3.b and little difference between the models can be found. Surprisingly, the integral width does not match the calculated cold work: it drops much more rapidly as a function of depth and does not show any sub-surface maximum. Only constrained plastic strain (and hence cold work) causes residual strains. Near surface unconstrained plastic flow may result in the highest integral width at the surface and decrease with depth. Whereas the maximum cold work calculated would occur at the depth where the plastic strains become constrained, hence subsurface, the dislocation density can well be higher at the very surface. In fact, not all the plastic work may contribute to the increase of the defect and dislocation density, microstresses or subgrain formation, which are causes of an increase in diffraction peak integral width.

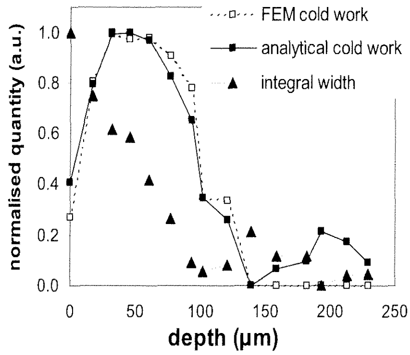

Fig.4. The normalised diffraction peak integral width and cold works calculated with the two models proposed in the text.

CONCLUSIONS

Two simple theoretical models were proposed to calculate the plastic strain necessary to introduce a measured residual stress profile in shot-peened Udimet 720Li. They used FEM and analytical conditions, working in reverse from the interpolated experimental data. Results show that both models predict a bell-shaped eigenstrain distribution of similar magnitude and shape. The tensile RS peak has been shown not to be a geometric effect, but generated by compressive plastic strain. The cold work calculated using the analytical model does not agree with the measured peak integral width profile. This suggests that unconstrained plastic flow occurs at the near surface and that not all plastic work causes changes that result in peak broadening.

ACKNOWLEDGEMENTS

One of the authors (MS) thanks the ILL, Grenoble, France, for funding to carry out this project. The experimental X-ray data were supplied by S.B.Kim and funded by Rolls-Royce Plc. We thank warmly Prof.T.Mori, who inspired the analytical approach.

REFERENCES

[Ezeilo, 2003] A.Ezeilo, in '*Analysis of Residual Stress by Diffraction using Neutron and Synchrotron Radiation*', ed. by M.E.Fitzpatrick and A.Lodini, Taylor &Francis, 2003, 251-262

[Korsunsky, 1997] A.M. Korsunsky, Proc. of International conference for residual stress, Linköping, Sweden, 1997, 275-280

[http, 2000], http://users.ox.ac.uk/~engs0161/gear.html

[Kim, 2004] S-B. Kim, A.D. Evans, J. Shackleton, G.Bruno, M. Preuss, P.J Withers, accepted for publication in Met.Trans.A

[Meguid, 2002] S.A. Meguid, G. Shagal, J.C. Stranart, Int. J. of Impact Eng. 27, 119-134, 2002

[Meguid, 1999] S.A. Meguid, G. Shagal, J.C. Stranart, J. Daly, Finite Elements in Analysis and Design, 31, 179-191, 1999

[Menig, 2003] R.,Menig, L.Pintschovius, V.Schulze, O.Vöhringer, Scripta Mater. 45, 977-983, 2003

[Noyan, 1987] I.C Noyan and J.B Cohen, Residual Stress: Measurement by Diffraction and Interpretation, Springer-Verlag, New York, 1987

[Schiffer, 1999] K. Schiffer, C. Droste gen. Helling, Computers and Structures 72, 329-340, 1999